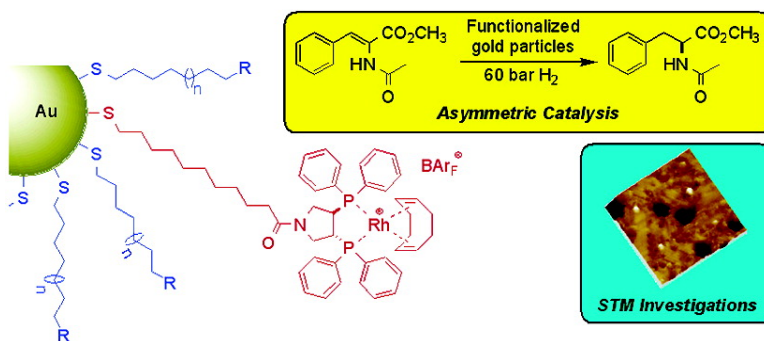


Immobilization of Rhodium Complexes at Thiolate Monolayers on Gold Surfaces: Catalytic and Structural Studies

Thomas Belser, Meike Sthr, and Andreas Pfaltz

J. Am. Chem. Soc., **2005**, 127 (24), 8720-8731 • DOI: 10.1021/ja0500714 • Publication Date (Web): 25 May 2005

Downloaded from <http://pubs.acs.org> on March 25, 2009



More About This Article

Additional resources and features associated with this article are available within the HTML version:

- Supporting Information
- Links to the 15 articles that cite this article, as of the time of this article download
- Access to high resolution figures
- Links to articles and content related to this article
- Copyright permission to reproduce figures and/or text from this article

[View the Full Text HTML](#)



Immobilization of Rhodium Complexes at Thiolate Monolayers on Gold Surfaces: Catalytic and Structural Studies

Thomas Belser,[†] Meike Stöhr,^{*‡} and Andreas Pfaltz^{*†}

Contribution from the Department of Chemistry, St. Johanns-Ring 19, and Department of Physics, Klingelbergstrasse 82, University of Basel, 4056 Basel, Switzerland

Received January 6, 2005; E-mail: Meike.Stoehr@unibas.ch; Andreas.Pfaltz@unibas.ch

Abstract: Chiral rhodium-diphosphine complexes have been incorporated into self-assembled thiolate monolayers (SAMs) on gold colloids. Catalysts of this type are of interest because they combine properties of homogeneous and heterogeneous systems. In addition, it should be possible to influence the catalytic properties of the metal center by the neighboring thiolate molecules. Colloids with a diameter of ca. 3 nm, coated with a mixed monolayer of *n*-octanethiolates and thiolates with chiral rhodium-PYRPHOS end groups, were studied as hydrogenation catalysts. With methyl α -acetamido-cinnamate as substrate, virtually the same enantioselectivities (up to 93% ee) and full conversion were obtained as with the corresponding homogeneous [Rh(COD)(PYRPHOS)]BAR_F catalyst. The colloids were easily recovered by filtration and reused as catalysts three times without loss of enantioselectivity. STM studies of analogous SAMs on Au(111) gave a detailed picture of the structure and dynamics of mixed monolayers of this type. The STM images showed that the catalyst-bearing thiolates are distributed statistically on the surface and that the ordered structure of the *n*-octanethiolate SAM can be retained during incorporation of the catalyst-bearing thiols using the place-exchange methodology.

Introduction

Both homogeneous and heterogeneous catalysts have their specific advantages and disadvantages. Heterogeneous catalysts can be easily recovered and recycled and are therefore ideal for industrial processes. However, our understanding of how such catalysts work is still insufficient, making the development of new catalysts very challenging. Moreover, no general methods are available for the preparation of defined metal surfaces with particular catalytic properties. In contrast to heterogeneous catalysis, the mechanism of homogeneous catalytic reactions is often known in detail. By means of a proper ligand, the reactivity and selectivity of a catalytic metal center can be tuned. However, separation from the reaction mixture and recycling is generally difficult.

To overcome this problem, homogeneous catalysts have been immobilized on solid supports such as organic polymers or inorganic solids.¹ Ideally, the support allows easy separation and recycling of the catalyst, but does not affect the catalytic process. Interesting extensions of this concept were reported by Tremel,² Mrksich,³ and Sasai,⁴ who attached transition-metal

complexes to self-assembled monolayers (SAMs) of alkanethiolates on gold colloids. The catalytic properties of these functionalized colloids were similar to those of the corresponding homogeneous catalysts.

SAMs of this type offer unique opportunities in catalysis, which have not been fully exploited yet. As illustrated in Figure 1, they can combine the properties of heterogeneous and homogeneous catalysts as well as enzymes. In contrast to conventional supported catalysts, the metal centers (M) can be embedded in an ordered monolayer of thiolate spacers (A), which can interact with the substrate (S) and in this way influence the reactivity and selectivity of a catalytic process.⁵ Depending on the chain length of the neighboring thiolates, two different classes of catalysts seem possible.

In one case a convex catalytic site is formed, resembling a homogeneous metal catalyst. Using appropriately functionalized neighboring thiolates, it should be possible to create specific binding sites for the substrate (e.g., hydrogen-bond donors or ionic groups). In addition, by separating the metal centers, the formation of aggregates between two or more metal complexes should be prevented. For reactions suffering from catalyst deactivation by aggregation, this should have a beneficial effect.

If the metal centers are located inside the monolayer formed by the neighboring thiolates, the active site has a concave structure similar to an enzyme. In this way catalysts can be constructed that should behave like hybrids of homogeneous and enzymatic catalysts. When the catalytic site (M) is sur-

[†] Department of Chemistry.

[‡] Department of Physics.

- (1) (a) Pugin, B.; Blaser, H.-U. In *Comprehensive Asymmetric Catalysis*; Jacobsen, E. N.; Pfaltz, A.; Yamamoto, H., Eds.; Springer: Berlin, 1999; Vol. III, pp 1367–1375. (b) Leadbeater, N. E.; Marco, M. *Chem. Rev.* **2002**, *102*, 3217. (c) Fan, Q.-H.; Li, Y.-M.; Chan, A. S. C. *Chem. Rev.* **2002**, *102*, 3385. (d) Song, C. E.; Lee, S. *Chem. Rev.* **2002**, *102*, 3495. (e) McMorn, P.; Hutchins, G. H. *Chem. Soc. Rev.* **2004**, *33*, 108.
- (2) Bartz, M.; Küther, J.; Seshadri, R.; Tremel, W. *Angew. Chem.* **1998**, *110*, 2646.
- (3) Li, H.; Luk, Y.-Y.; Mrksich, M. *Langmuir* **1999**, *15*, 4957.
- (4) Marubayashi, K.; Takizawa, S.; Kawakusu, T.; Arai, T.; Sasai, H. *Org. Lett.* **2003**, *23*, 4409.

- (5) For a similar approach based on bifunctionalized mesoporous silica, see: Huh, S.; Chen, H.-T.; Wiench, J. W.; Pruski, M.; V. Lin, S.-Y. *J. Am. Chem. Soc.* **2004**, *126*, 1010.

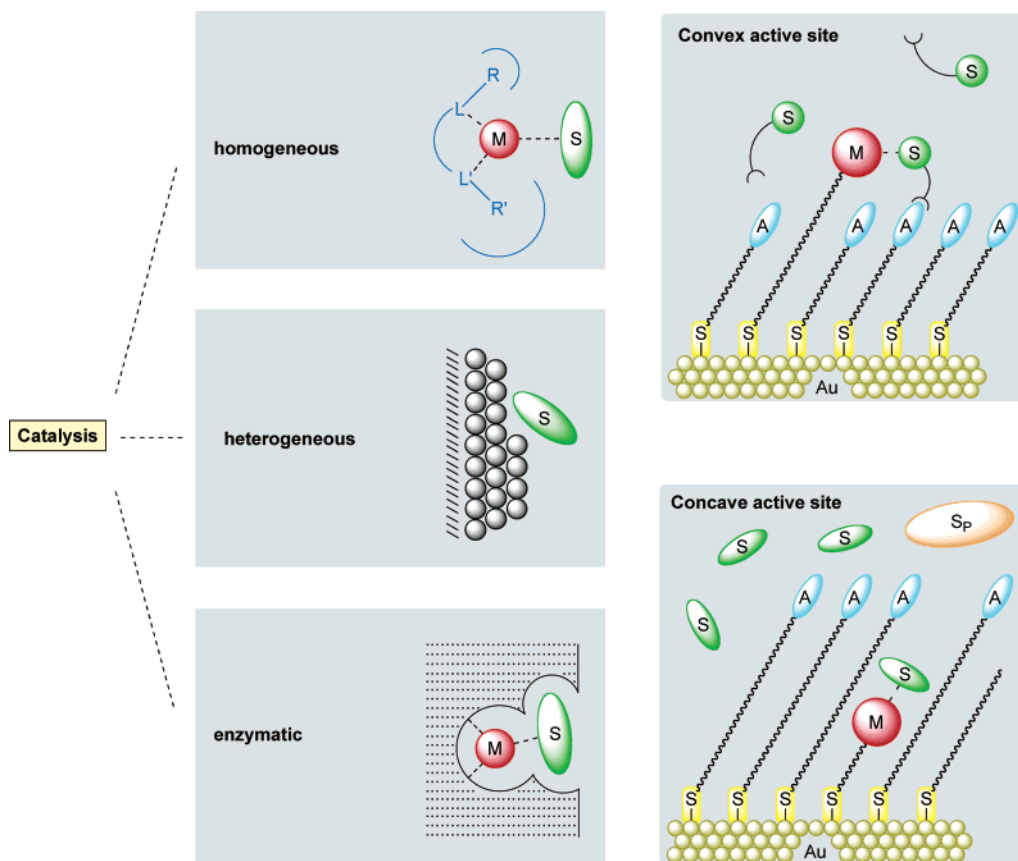


Figure 1. Comparison of homogeneous, heterogeneous, and enzymatic catalysts (left) and schematic representations of metal catalysts attached to thiolate monolayers on gold surfaces (right).

rounded by apolar alkyl chains, a selective reaction of nonpolar substrates (S) in the presence of polar substrates (S_p) should be possible. By modification of the neighboring thiolates, the environment of the metal center can be readily changed and, if desired, specific binding sites for the substrate can be introduced.

To explore these possibilities, we decided to prepare mixed SAMs on gold surfaces containing alkanethiolates with chiral rhodium catalysts as terminal groups.⁶ As a test reaction we chose the rhodium-catalyzed asymmetric hydrogenation of enamides, which is mechanistically well understood and, therefore, ideal for this purpose.^{7–9}

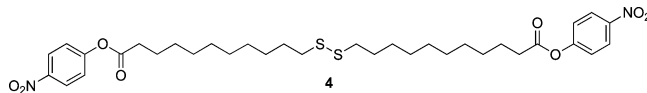
We herein report the preparation and catalytic studies of mixed monolayers of alkanethiolates and thiolates functionalized with rhodium-diphosphine complexes. We also present the results of STM analyses of SAMs on (111)-Au surfaces, which reveal a detailed picture of the structure and dynamics of mixed monolayers of this type.

Results and Discussion

Preliminary Investigations with Gold Particles. Initial experiments were carried out using gold particles with an average diameter of 0.3–3 μm, which were covered with a

monolayer of alkanethiolate chains bearing chiral rhodium complexes as end groups (Scheme 1). The chiral diphosphine ligand PYRPHOS was chosen,¹⁰ since it can be easily attached to a linker through an amide bond, as shown in structure 1. To functionalize the gold surface, we treated the gold particles in dichloromethane at 23 °C with disulfide 1, which was readily prepared from 11-(10'-carboxydecyl)undecanoic acid via the acid chloride (see Supporting Information). The diphosphine-covered particles 2 were then treated with [Rh(COD)-Cl]₂ (COD = 1,5-cyclooctadiene) and TIBAr_F^{11,12} (BAr_F = tetrakis[3,5-bis(trifluoromethyl)phenyl]borate) to give the functionalized particles 3.

The surface coverage with thiolate molecules, typically obtained under these conditions, was determined by means of disulfide 4 bearing *p*-nitrophenyl ester end groups. After immobilization, the *p*-nitrophenyl ester groups were hydrolyzed by treatment under basic conditions (dioxane/1 M NaOH_(aq) solution 1:1 (v/v)) and the concentration of *p*-nitrophenolate was measured by UV/vis spectroscopy. After an incubation time of 24 h using a disulfide concentration of 0.05 M in dichloromethane at 23 °C, the thiolate content of the gold particles was found to be 1.87 × 10⁻⁶ mol *p*-nitrophenyl ester per gram gold particles.



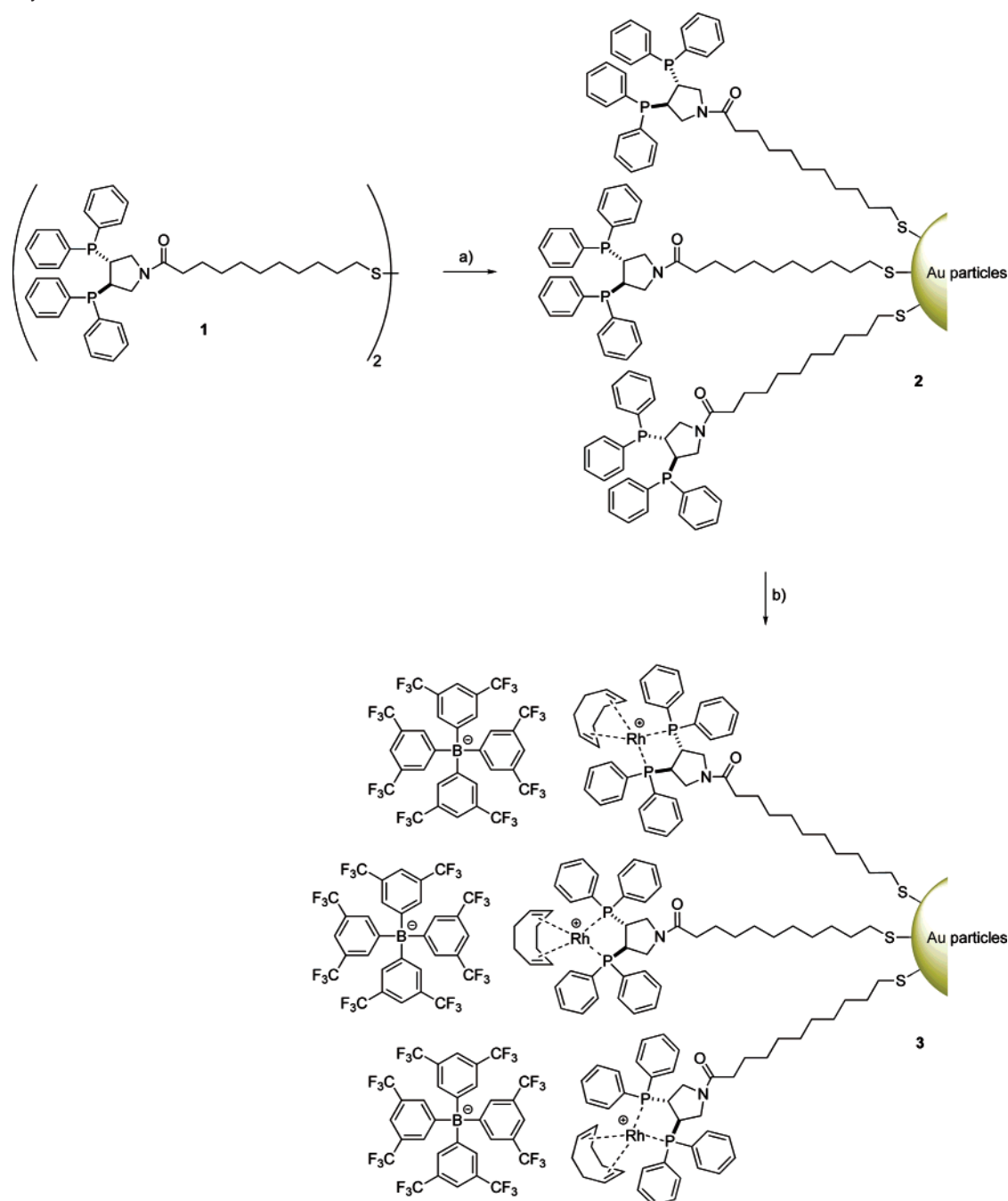
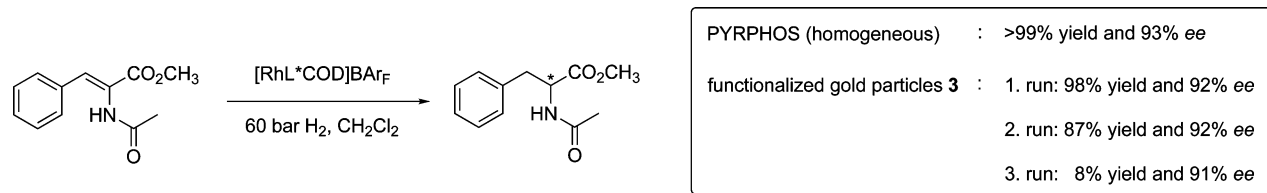
The functionalized gold particles 3 containing rhodium-PYRPHOS end groups were tested as catalysts in the hydro-

(6) Incorporation of a Rh catalyst into LB films: Töllner, K.; Popovitz-Biro, R.; Lahav, M.; Milstein, D. *Science* **1997**, *278*, 2100.

(7) Landis, C. R.; Halpern, J. *J. Am. Chem. Soc.* **1987**, *109*, 1746.

(8) (a) Brown, J. M. In *Comprehensive Asymmetric Catalysis*; Jacobsen, E. N.; Pfaltz, A.; Yamamoto, H., Eds.; Springer: Berlin, 1999; Vol. I, pp 121–182. Gridnev, I. D.; Imamoto, T. *Acc. Chem. Res.* **2004**, *37*, 633. (b) Gridnev, I. D.; Imamoto, T. *Acc. Chem. Res.* **2004**, *37*, 633.

(9) (a) Landis, C. R.; Hilfenhaus, P.; Feldgus, S. *J. Am. Chem. Soc.* **1999**, *121*, 8741. (b) Feldgus, S.; Landis, C. R. *J. Am. Chem. Soc.* **2000**, *122*, 12714.

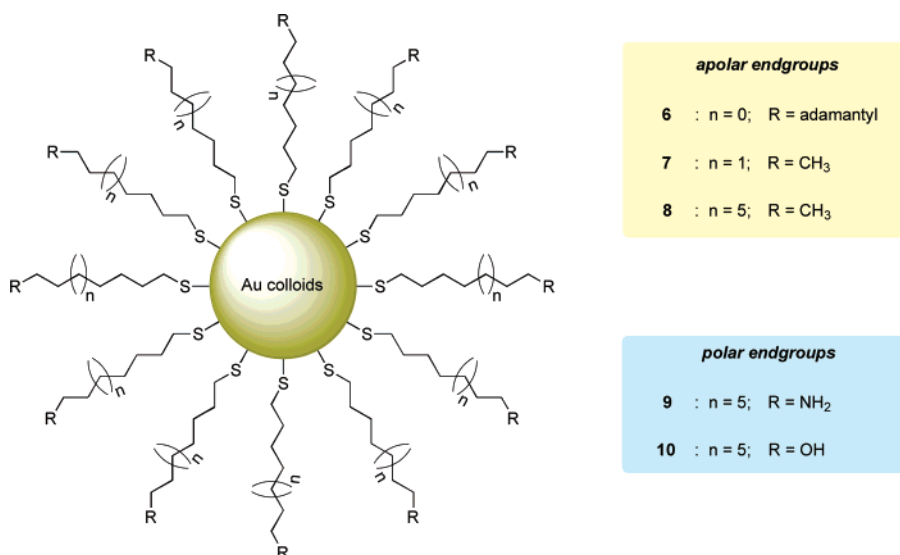
Scheme 1. Synthesis of Functionalized Gold Particles **3**^a**Scheme 2.** Asymmetric Hydrogenation of Methyl α -Acetamidocinnamate

genation of methyl α -acetamidocinnamate (Scheme 2). The reactions were carried out in dichloromethane under 60 bar of

hydrogen pressure. For 1 mmol of olefin, 11 g of gold particles **3** were used, which was equivalent to approximately 1–2 mol % of rhodium catalyst. For comparison, the analogous homo-

(10) (a) Nagel, U. *Angew. Chem.* **1984**, *96*, 425. (b) Nagel, U.; Kinzel, E.; Andrade, J.; Prescher, G. *Chem. Ber.* **1986**, *119*, 3326.
 (11) Brookhart, M.; Grant, B.; Volpe, A. F. *Organometallics* **1992**, *11*, 3920.

(12) Hughes, R. P.; Lindner, D. C.; Rheingold, A. L.; Yap, G. P. A. *Inorg. Chem.* **1997**, *36*, 1726.

Scheme 3. Apolar and Polar Alkanethiolate-Protected Gold Colloids

geneous reaction was carried out under the same conditions, using 2 mol % of the rhodium complex derived from *N*-octanoyl-PYRPHOS as catalyst.

The immobilized rhodium-PYRPHOS catalyst proved to be active and showed virtually the same enantioselectivity as the analogous homogeneous catalyst. The gold particles could be recycled, giving the same ee values with only slightly reduced yields in the second run. In the third run, however, low yields were obtained due to deactivation of the catalyst. The reaction solution in these experiments was colorless and did not contain any phosphorus compounds according to ³¹P NMR analysis, ruling out catalyst leaching under the reaction conditions. Deactivation is a common phenomenon observed upon recycling of immobilized catalysts, which may be caused, for example, by undesired reactions of the highly reactive Rh centers with oxygen or other impurities during catalyst recovery.¹

Our results demonstrate that rhodium-diphosphine hydrogenation catalysts can be immobilized on thiolate monolayers attached to gold surfaces and that the immobilized complexes retain their catalytic activity and enantioselectivity. However, for full conversion, a relatively large quantity of gold particles (11 g/mmol of substrate) has to be used. Experiments with mixed monolayers consisting of functionalized thiolates surrounded by an excess of nonfunctionalized spacers would require even larger amounts of gold, making such studies impractical. Therefore, we decided to investigate immobilization on gold colloids, which are 2–3 orders of magnitude smaller than the functionalized gold particles **3** (2–10 nm vs 300–3000 nm) with far higher surface area per unit mass.

Functionalized Gold Colloids. A series of *n*-alkanethiolate-protected gold colloids with diameters between 2.3 and 3.5 ± 0.6 nm were prepared using a modified procedure of Murray and co-workers.¹³ An aqueous solution of hydrogen tetrachloroaurate was extracted into toluene and metathesized to the tetraoctylammonium salt in the presence of a toluene solution of tetraoctylammonium bromide. To this organic solution was added *n*-alkanethiol, followed by an aqueous solution of sodium borohydride. Reduction of the gold salt and concomitant derivatization by *n*-alkanethiol was evidenced by prompt

darkening of the toluene phase. After stirring for 12 h, the toluene layer was separated, concentrated, and diluted with ethanol. The thiolate-protected colloids were isolated by precipitation at –60 °C. In addition to 6-(adamant-1-yl)hexanethiol, *n*-octanethiol, and *n*-dodecanethiol, 11-aminoundecane-1-thiol or 11-mercaptoundecan-1-ol was used as polar thiolate to protect the colloids. The apolar colloids **6–8** were purified by precipitation from toluene with ethanol, whereas the polar colloids **9** and **10**, which precipitated from the reaction mixture, were isolated by filtration and washed several times with diethyl ether to remove any residual thiols (Scheme 3).

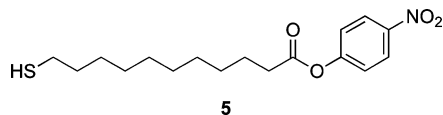
The colloids were characterized by elemental analysis and TEM, which visualized the gold core. From the results, the molecular weight and thiolate surface coverage were estimated on the basis of a structural model of the gold core shape. The spherical model employed approximates the gold core as a sphere, covered with a skin of hexagonally close-packed gold atoms.^{14–17} According to this model, colloid **7** with an average diameter of 3.48 ± 0.61 nm contains 1298 gold atoms and 211 adsorbed octanethiolates on the surface. Gold colloids (**8–10**) with sterically nondemanding end groups gave similar results, whereas the gold colloid **6** with an average diameter of 2.32 ± 0.46 nm, bearing bulky adamantyl end groups, contained only 385 gold atoms and 68 adsorbed thiolates. Thermogravimetric analysis and XPS measurements showed that the S–Au bonds are stable up to 150 °C. The colloids were also stable under the conditions of the hydrogenation reactions described below (4 h, 23 °C at 60 bar of H₂ with mechanical stirring). Leaching of adsorbed thiolates after 24 h at 100 bar of H₂ was less than 0.2% (GC analysis of the reaction solution). Thus, these protected gold colloids served as convenient precursors for the incorporation of rhodium-diphosphine complexes into the thiolate monolayer.

Various methods have been described for introducing functional components into SAMs of thiolates on gold surfaces.¹⁸

(13) Hostetler, M. J., et al. *Langmuir* **1998**, *14*, 17.

(14) D'Agostino, G.; Pinto, A.; Mobilio, S. *Phys. Rev. B* **1993**, *48*, 14447.
 (15) Sellers, H.; Ulman, A.; Shnidman, Y.; Eilers, J. E. *J. Am. Chem. Soc.* **1993**, *115*, 9389.
 (16) Whetten, R. L.; Gelbart, W. M. *J. Phys. Chem.* **1994**, *98*, 3544.
 (17) Leff, D. V.; Ohara, C.; Heath, J. R.; Gelbart, W. M. *J. Phys. Chem.* **1995**, *99*, 7036.

In our case, we chose the place-exchange reaction^{19,20} for the preparation of mixed monolayers containing the chiral rhodium catalysts, because of its simplicity and versatility. Moreover, this method allows functionalization of colloids without altering their dimensions.



Initial experiments were carried out with the *p*-nitrophenyl-ester-bearing thiol **5**, to determine the extent of thiolate exchange in relation to the reaction time under specific conditions. After incubation of the *n*-octanethiolate-protected colloids **7** in a solution of **5** in dichloromethane, the resulting functionalized colloids were separated by filtration with a solvent-resistant stirred cell and isolated as a black solid after precipitation from ethanol/hexanes at $-60\text{ }^{\circ}\text{C}$. The ratio between functionalized thiolates and *n*-octanethiolates in the SAMs could be deduced from ^1H NMR spectra of the colloids. The concentration of nitrophenyl esters per gram of gold was determined by UV/vis spectroscopy after basic hydrolysis. After incubation in a 1.5 mM solution of thiol in dichloromethane for 24 h at $23\text{ }^{\circ}\text{C}$, a ratio of 4.4:1 between *n*-octanethiolate and the *p*-nitrophenyloxycarbonyl-substituted thiolate and a concentration of 0.15 mmol of nitrophenylester per gram of gold colloids was found. Longer incubation times or higher concentration of thiol **5** resulted in lower *n*-octanethiolate/functionalized thiolate ratios (an incubation time of 48 h at $23\text{ }^{\circ}\text{C}$ resulted in a 2:1 ratio between *n*-octanethiolate and the *p*-nitrophenyloxycarbonyl-substituted thiolate). Virtually identical results were obtained in dichloromethane or ethanol.

Exchange with the rhodium-PYRPHOS-bearing thiol **12** was carried out in the same manner. The resulting functionalized gold colloids **13–17** were purified by precipitation from ethanol with hexanes and analyzed by TEM and ^1H NMR spectroscopy. The TEM studies revealed that the size of the gold core did not significantly change during the place-exchange reaction. The content of functionalized thiolates **12** in the mixed SAMs, determined by ^1H NMR spectroscopy, was strongly dependent on the nature of the thiolates in the precursor colloids **6–10** and the incubation time. An incubation time of 48 h at $23\text{ }^{\circ}\text{C}$ led to a 1:1–2:1 ratio between rhodium-PYRPHOS-containing thiolates and the surrounding spacer thiolates. For our catalytic studies, we wanted to use SAMs consisting of rhodium complexes separated by excess spacer thiolates. Therefore, we reduced the incubation time to 24 h, resulting in a 1:3–1:8 rhodium-PYRPHOS/spacer ratio (Scheme 4).

The functionalized gold colloids **13–17** were tested as catalysts in the hydrogenation of methyl α -acetamidocinnamate. The apolar colloids **13–15** with *n*-octanethiolate, 6-(adamant-1-yl)hexanethiolate, and *n*-dodecanethiolate as spacers were all found to be highly active catalysts, giving high conversion and good enantioselectivities similar to the corresponding homogeneous reaction using $[\text{Rh}(\text{COD})(\text{octanoyl-PYRPHOS})]\text{BARf}$ as

catalyst. The polar colloids **16** and **17** with amino and hydroxy end groups proved to be less reactive and less enantioselective (Table 1). Although no satisfactory explanation for the observed negative effects of the amino and hydroxy groups can be given at this stage, the results show that the spacer end groups can strongly influence the performance of the catalyst.

After separation of the colloids, the reaction solutions were analyzed by ^{31}P NMR spectroscopy. The lack of any ^{31}P signals implied that no catalyst leaching was occurring. This was also confirmed by elemental analysis (Rh, P, S). The particle size of the recovered colloids was checked by TEM and found to be the same as before the hydrogenation reaction.

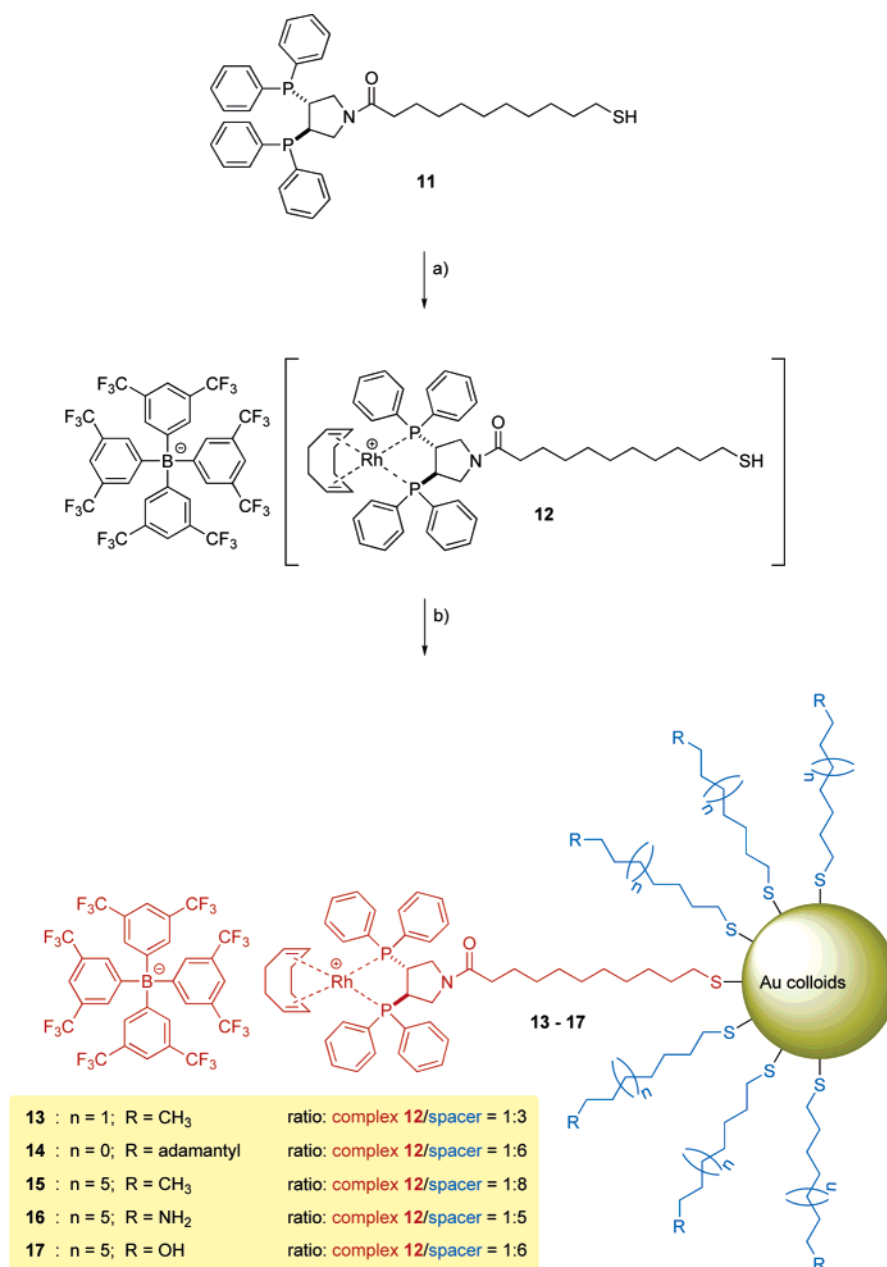
Furthermore, recycling of the functionalized gold colloids **13** was investigated. After the reaction, the colloids were treated immediately with 10 equiv of COD to restore the original rhodium complex. The colloids could be readily recovered by filtration using centrifugal filter units with a cutoff molecular size of 50 kD and were successfully used again as catalysts. The enantioselectivities remained constant during three recycling steps, while conversion decreased moderately from 99% to 74% in the fourth cycle (standard reaction time: 4 h). However, if the reaction time was increased to 12 h, almost full conversion could be obtained even in the third cycle (96% vs 86% after 4 h).

STM Investigations. To obtain detailed structural information on the arrangement of the ionic catalysts **12** embedded in an *n*-octanethiolate matrix and to get a better understanding of the exchange process itself, STM measurements were conducted. An important question was whether the catalyst molecules were clustered or distributed statistically on the gold surface. For the STM investigations (111)-oriented gold films were chosen, as it has been found by different analytical techniques such as XRD (X-ray diffraction), XPS (X-ray photoelectron spectroscopy), IR spectroscopy, and solid-state NMR spectroscopy^{2,21} that the properties of planar surfaces and gold colloids covered with a SAM are very similar (for an exception see ref 22). Especially, the Au–S bonding and chain ordering are essentially the same for both systems. Nevertheless, there are also differences that should be kept in mind: the curvature of the colloid surface and the higher concentration of defectlike sites on the colloids, which explains the higher density of alkanethiolates on gold colloids compared to flat surfaces. However, mechanistic studies of place-exchange reactions at colloid and Au(111) surfaces have shown that, although the reaction rates may differ, the basic mechanism is the same for the two systems.²³ Thus we assume that STM results obtained on flat surfaces after the exchange reaction are also relevant for the corresponding gold colloids.

For our studies, an upright standing arrangement of the thiolates was required, to obtain comparable initial conditions

- (18) Brust, M.; Fink, J.; Bethell, D.; Schiffrin, D. J.; Kiely, C. *J. Chem. Soc., Chem. Commun.* **1995**, 1655.
 (19) Hostetler, M. J.; Green, S. J.; Stokes, J. J.; Murray, R. W. *J. Am. Chem. Soc.* **1996**, *118*, 4212.
 (20) Ingram, R. S.; Hostetler, M. J.; Murray, R. W. *J. Am. Chem. Soc.* **1997**, *119*, 9175.

- (21) (a) Whetten, R. L.; Khoury, J. T.; Alvarez, M. M.; Murthy, S.; Vezmar, I.; Wang, Z. L.; Stephens, P. W.; Cleveland, C. L.; Luedtke, W. D.; Landman, U. *Adv. Mater.* **1996**, *8*, 428. (b) Hostetler, M. J.; Stokes, J. J.; Murray, R. W. *Langmuir* **1996**, *12*, 3604. (c) Badia, A.; Cuccia, L.; Demers, L.; Morin, F.; Lennox, R. B. *J. Am. Chem. Soc.* **1997**, *119*, 2682. (d) Bourg, M.-C.; Badia, A.; Lennox, R. B. *J. Phys. Chem. B* **2000**, *104*, 6562. (e) Li, X.-M.; Huskens, J.; Reinhoudt, D. N. *J. Mater. Chem.* **2004**, *14*, 2954.
 (22) Jackson, A. M.; Myerson, J. W.; Stellacci, F. *Nat. Mater.* **2004**, *3*, 330. In this case, mixtures of alkanethiolates and thiolates with carboxylic acid or arylamino headgroups were found to form phase-separated ordered domains on colloids, whereas disordered domains were observed on flat surfaces. In our case, the functionalized thiolates showed no apparent tendency to aggregate.
 (23) (a) Hostetler, M. J.; Templeton, A. C.; Murray, R. W. *Langmuir* **1999**, *15*, 3782. (b) Donkers, R. L.; Song, Y.; Murray, R. W. *Langmuir* **2004**, *20*, 4703. (c) Ionita, P.; Caragheorghopol, A.; Gilbert, B. C.; Chechik, V. *Langmuir* **2004**, *20*, 11536.

Scheme 4. Synthesis of Functionalized Gold Colloids 13–17^a

^a (a) [Rh(COD)Cl]₂, TIBA_{TP},^{11,12} CH₂Cl₂, 52%. (b) Gold colloids (2 mg/mL), 1.5 mM solution of rhodium complex 12, CH₂Cl₂, 24 h, 23 °C.

and reproducible experiments and to ensure that an exchange reaction was taking place rather than an adsorption process, which could occur if the thiolate molecules were lying parallel to the surface. Therefore, the different experimental parameters required for obtaining the desired upright SAM were investigated in more detail using *n*-octanethiol.

Comparing different solvents (see Experimental Section) while the immersion time, temperature, and thiol concentration were kept constant, we found that ethanol and dichloromethane gave the best results. The ordering of the SAMs was reached faster in either ethanol or dichloromethane in comparison to acetone or diethyl ether. Furthermore, the concentration, immersion time, and temperature were varied for ethanol and dichloromethane. If the concentration was in the mM range, an immersion time of at least 24 h was needed to form an upright SAM. By increasing the concentration to 0.1 M, the immersion

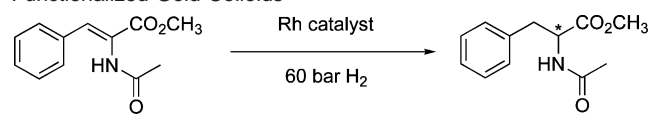
time could be reduced to 8 h. Finally, the solution temperature was increased from 23 to 55 °C, resulting in larger domains and fewer etch pits.²⁴ On the basis of these results, a thiol concentration of 0.1 M in ethanol or dichloromethane and an immersion time of 8 h at 55 °C were chosen as standard conditions for subsequent experiments. Figure 2 shows a typical STM image for the upright standing hexagonal ($\sqrt{3} \times \sqrt{3}$)R30 thiolate arrangement on Au(111) obtained under these conditions.^{25,26}

When the sample was kept under ambient conditions for several days, a different arrangement of *n*-octanethiolate on Au(111) was observed (Figure 3). To date, a structure of this type was reported only once and was described as the thermody-

(24) Delamarche, E.; Michel, B.; Gerber, C.; Anselmetti, D.; Güntherodt, H.-J.; Wolf, H.; Ringsdorf, H. *Langmuir* **1994**, *10*, 2869.

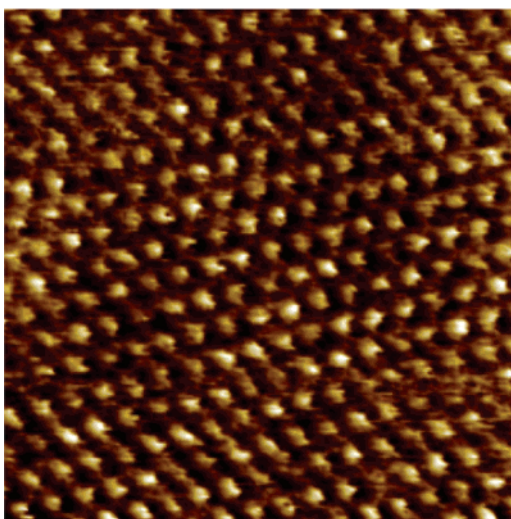
(25) Widrig, C. A.; Alves, C. A.; Porter, M. D. *J. Am. Chem. Soc.* **1991**, *10*, 2805.

(26) Poirier, G. E.; Tarlov, M. J. *Langmuir* **1994**, *10*, 2853.

Table 1. Hydrogenation of Methyl α -Acetamidocinnamate with Functionalized Gold Colloids^a


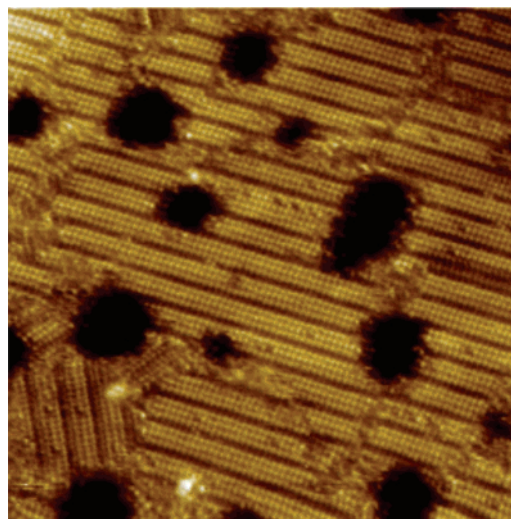
colloid ^a	solvent	spacer/[Rh] ^b	conversion (%) ^c	ee (%) ^d
13 (30 mg)	CH ₂ Cl ₂	1:3	>99 [>99]	93 [93]
13 (30 mg)	EtOH	1:3	84 [61]	87 [88]
14 (50 mg)	CH ₂ Cl ₂	1:6	>99 [>99]	93 [93]
14 (50 mg)	EtOH	1:6	91 [61]	88 [88]
15 (60 mg)	CH ₂ Cl ₂	1:8	>99 [>99]	92 [93]
15 (60 mg)	EtOH	1:8	81 [61]	87 [88]
16 (60 mg)	CH ₂ Cl ₂	1:5	94 [>99]	86 [93]
16 (60 mg)	EtOH	1:5	20 [61]	82 [88]
17 (60 mg)	CH ₂ Cl ₂	1:6	32 [>99]	82 [93]
17 (60 mg)	EtOH	1:6	12 [61]	68 [88]

^a Conditions: 110 mg (0.50 mmol) of substrate in 1 mL of solvent, ca. 1 mol % of [Rh], 23 °C, 4 h, 60 bar of H₂, stirring rate 600 rpm. ^b Determined by ¹H NMR analysis. ^c Determined by GC (Restek Rtx-1701); the values in brackets correspond to the homogeneous reaction using [Rh(COD)(*n*-octanoyl-PYRPHOS)]BARf. ^d Determined by HPLC (Daicel Chiralcel OD-H); the values in brackets correspond to the homogeneous reaction using [Rh(COD)(*n*-octanoyl-PYRPHOS)]BARf.

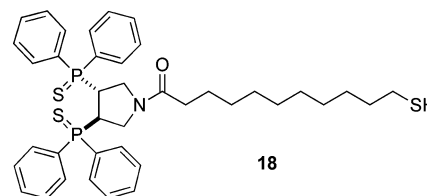
**Figure 2.** STM image of *n*-octanethiolates on Au(111) in the ($\sqrt{3} \times \sqrt{3}$)-R30 arrangement (8 nm \times 8 nm, -1 V, 16 pA). The gold substrate was immersed for 8 h in 0.1 M *n*-octanethiol solution in ethanol at 55 °C.

namically favored arrangement.²⁷ This structural change is explained by the transformation of the hexagonal ($\sqrt{3} \times \sqrt{3}$)-R30 arrangement into the ($6 \times \sqrt{3}$) arrangement, which involves both a motion of the sulfur headgroups to different sites on the Au(111) surface and a change of the tilt angle of the alkyl chains. In our case, the ($6 \times \sqrt{3}$) structure already emerged after 5 days compared to 6 months, as reported by Noh and co-workers.²⁷ In an earlier publication, a similar transformation of the ($\sqrt{3} \times \sqrt{3}$)-R30 into a ($5\sqrt{3} \times \sqrt{3}$) structure was reported.²⁸ This structure appeared after storing the sample for \sim 1 week in air. These findings show that the hexagonal ($\sqrt{3} \times \sqrt{3}$)-R30 arrangement, initially formed, is not stable over longer time periods and thus does not correspond to the thermodynamically favored structure.

Exchange Reaction with Ligand 18. For the first exchange experiments with *n*-octanethiolate SAMs, the metal-free thiolate

**Figure 3.** STM image of *n*-octanethiolates on Au(111) in the $p(6 \times \sqrt{3})$ arrangement (40 nm \times 40 nm, -0.95 V, 37 pA). The gold substrate was immersed for 8 h in 0.1 M *n*-octanethiol solution in ethanol at 23 °C and stored under ambient conditions for 5 days before the image was recorded.

18 rather than metal catalyst **12** was chosen in order to circumvent potential interactions of the tip with the ionic rhodium complex or the counterion and to gain information on the exchange reaction with the binary system. It has been shown that exchange reactions of this type are fast in the initial phase, but then slow significantly before they gradually reach equilibrium after 1–2 days.^{29–31}



Initially, conditions similar to those reported in the literature were used, with immersion times of the *n*-octanethiolate-coated sample in the solution of **18** between 24 and 48 h at 23 °C. Analysis of the resulting mixed SAMs with STM (not shown) showed a statistical distribution of protrusions, which could be ascribed to the functionalized thiolates **18**. The protrusions were surrounded by noisy regions, indicating that the ordered upright standing arrangement of the *n*-octanethiolate SAM had vanished. These findings suggested that a significant amount of *n*-octanethiolate was exchanged with ligand **18**, but in addition, a certain amount of thiolates were desorbed into the solution without being replaced by ligands **18**, resulting in partial destruction of the ordered SAM.³² Consequently, *n*-octanethiol was added to the solution of **18** to suppress desorption of thiolates, and the immersion time was reduced to 4 h. Under these conditions, the upright-standing ordered *n*-octanethiolate matrix was conserved, while the exchange reaction could take place.

A characteristic image of a sample prepared using this protocol is shown in Figure 4. The functionalized thiolates **18**

(27) Noh, J.; Hara, M. *Langmuir* **2002**, *18*, 1953.(28) Schönenberger, C.; Jorritsma, J.; Sondag-Huethorst, J. A. M.; Fokink, L. G. J. *J. Phys. Chem.* **1995**, *99*, 3259.(29) Chidsey, C. E. D.; Bertozzi, C. R.; Putvinski, T. M.; Mujisce, A. M. *J. Am. Chem. Soc.* **1990**, *112*, 4301.(30) Collard, D. M.; Fox, M. A. *Langmuir* **1991**, *7*, 1192.(31) Chung, C.; Lee, M. *J. Electroanal. Chem.* **1999**, *468*, 91.(32) Schlenoff, J. B.; Li, M.; Ly, H. *J. Am. Chem. Soc.* **1995**, *117*, 12528.

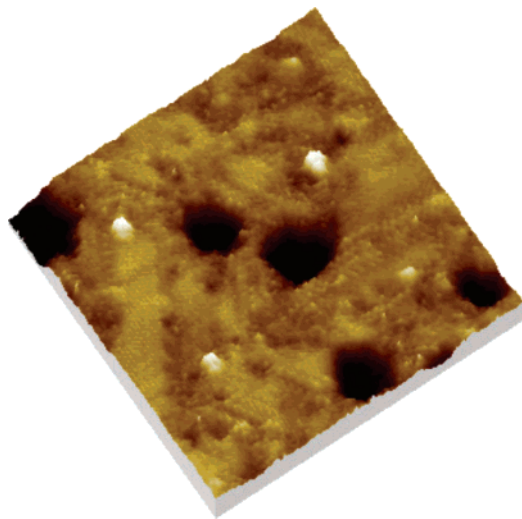


Figure 4. STM image of ligands **18** embedded in an *n*-octanethiolate matrix on Au(111) (33 nm × 33 nm, 1.2 V, 18 pA). The ligands appear as protrusions, and the height difference between the *n*-octanethiolates and the ligand **18** amounts to about 1.5–2.5 Å.

are distributed statistically and appear as bright protrusions with heights in the range 1.5–2.5 Å above the *n*-octanethiolate SAM. These values are considerably shorter than the theoretical value for the height difference (1.2 nm) if thiolate **18** exists in a stretched conformation. However, realistically much shorter values than 1.2 nm are expected, as the alkyl chain and the large headgroup are flexible and can bend to the side, placing themselves on top of neighboring *n*-octanethiolates.

Furthermore, it has to be kept in mind that STM does not show the real topography of a sample, especially for organic adsorbates on conducting substrates. By keeping the conductance constant as performed during constant current tunneling mode, the STM image displays the local density of states (LDOS) of the sample. Interpretation of the resulting image as a real topographical representation is only possible if the LDOS is uniform over the entire sample surface. Since we are dealing with two strongly different organic molecules immobilized on a metal surface, the LDOS above an *n*-octanethiolate and thiolate **18** are expected to differ substantially. For the headgroups of **18** an average diameter of about 2 nm was measured. It should be noted that the measured values for the individual molecules in the SAM varied between 1.2 and 2.6 nm and, moreover, the diameter for the same molecule was found to change from one image to the next. The observed deviation of the measured diameter from the theoretical value (1.2 nm) is not unexpected because the size of protrusions is always overestimated by scanning probe microscopy due to the geometric convolution of the tip shape and the adsorbate shape.^{33,34} Moreover, tilting of the headgroups is also likely to contribute to a seemingly enlarged diameter. Hence, we conclude that each protrusion represents a single molecule of thiolate **18**.

Exchange Reaction with Rhodium Catalyst **12.** For the exchange reaction of the *n*-octanethiol-covered gold substrates with the rhodium(diphosphine)-containing thiolate **12** an immersion time between 1 and 2 h was chosen. No additional *n*-octanethiol was added in order to avoid possible reactions with the rhodium complex. In contrast to the experiments with

thiolate **18** (see above), the ordered SAM was retained under these conditions. Again, a statistical distribution of the functionalized thiolates was observed. Figure 5 shows a time lapse series of STM images of a sample prepared in this way. The six images, which show the same area of the SAM, were taken at time intervals of 4 min. The bright protrusion represents one catalyst molecule **12** (annotated in red). It appears that in the sequences of images (a)–(f) the molecule is moving to the top; however, what is seen is in fact thermal drifting of the sample. Relative to the black arrow that indicates the same position in all six images, thiolate **12** does not move.

The catalyst molecules appear to overtop the *n*-octanethiolate SAM by 2–4 Å, whereas for the headgroup a diameter of 1–3 nm is measured. As observed for the analogous metal-free thiolate **18**, the value for the height difference is substantially smaller than the value expected for a static stretched geometry of the thiolate chain of **12** (1.2 nm). The values for both the diameter and the height are more disperse for the rhodium complex **12** than for thiolate **18**. In addition, scanning over **12** often resulted in noisy areas in the STM image. Before considering possible explanations for these observations, a more detailed analysis of Figure 5 should be made. The appearance of rhodium complex **12** changes from image to image with regard to diameter, height, and noise. In image (e) no protrusion is observed, although **12** must still be in the same place as confirmed by the successive image (f). Such a blinking behavior was also observed for other catalyst molecules **12** of the same sample and for different samples prepared in the same manner. A similar phenomenon was reported for phenylene-ethynylene oligomers embedded in a thiolate matrix by Donhauser and co-workers.³⁵ They ascribed this blinking to a switching in conductance caused by density changes of the surrounding matrix. In our case we interpret the blinking in the following way.

(i) So far, the ionic character of **12** has not been taken into account. In general, the role of the counterion on the STM image contrast is unclear because its position on the surface cannot be determined precisely. We assume that it must reside in close vicinity to the cationic rhodium complex to compensate its charge. If the counterion actually contributes to the image contrast, the observed diameter and/or height of **12** will vary depending on the position of the counterion. In addition, it is reasonable to assume that the ion pair is flexible with the counterion moving around in the vicinity of the rhodium complex. This movement could be at least partially responsible for the observed noisy tunneling current.

(ii) As discussed for thiolate **18**, the alkyl chain and the cationic headgroup of **12** are flexible and can tilt. If a repulsive interaction between tip and headgroup is assumed, the head will avoid the tip during scanning. As a consequence, this may result in a noisy tunneling current with no visible protrusion in the STM image. The interaction between the tip and the headgroup will depend on the electronic properties of the tip, which are strongly influenced by the configuration and material of the foremost atoms. These properties can alter considerably if the tip is picking up or releasing adsorbates during scans. In addition, the interaction will depend on the specific arrangement

(33) Klyachko, D.; Chen, D. M. *Surf. Sci.* **2000**, *446*, 98.

(34) G. Mark, I.; L. Biro, P.; Gyulai, J. *Phys. Rev. B* **1998**, *58*, 12645.

(35) Donhauser, Z. J.; Mantooh, B. A.; Kelly, K. F.; Bumm, L. A.; Monnell, J. D.; Stapleton, J. J.; Price, D. W.; Rawlett, A. M.; Allara, D. L.; Tour, J. M.; Weiss, P. S. *Science* **2001**, *292*, 2303.

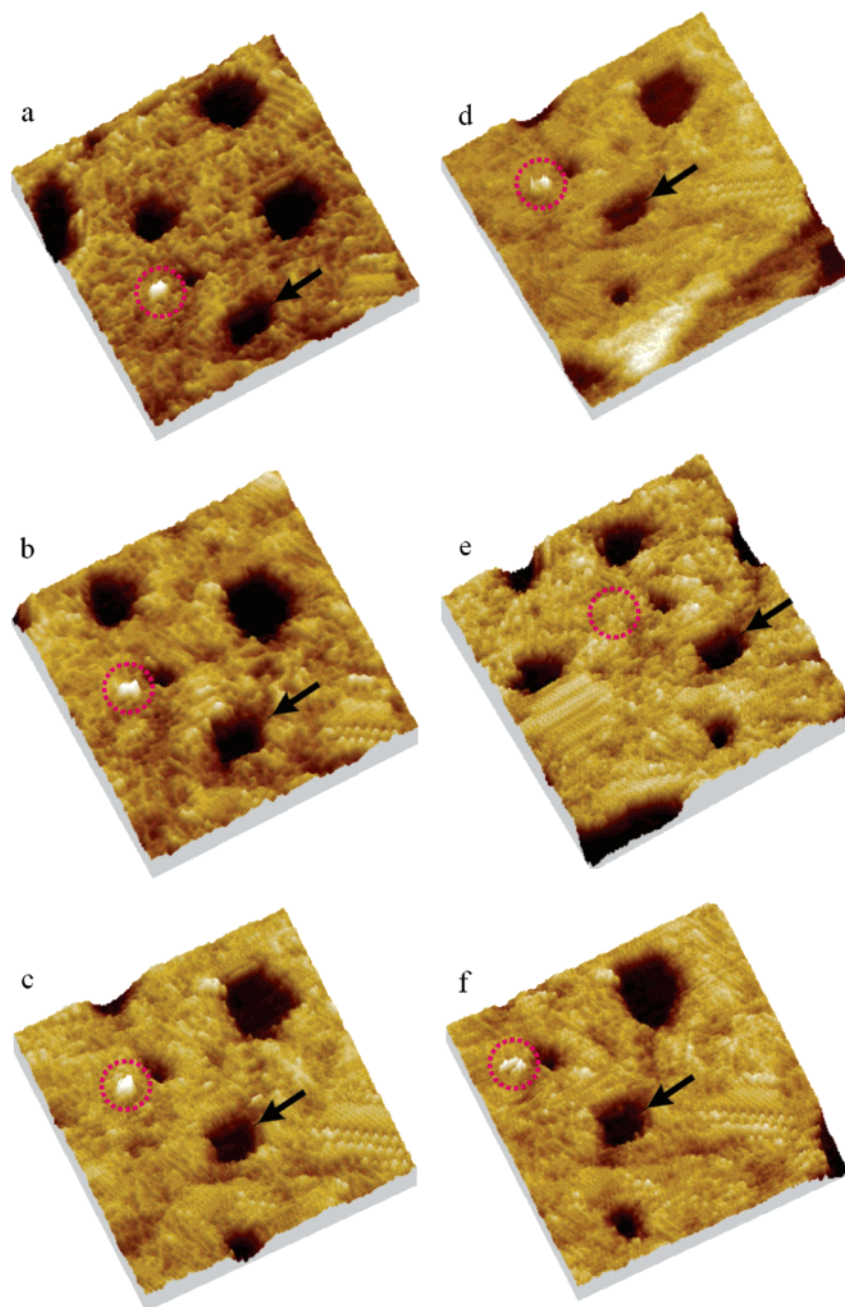


Figure 5. Time lapse series of STM images of the same sample area showing one catalyst **12** (encircled in red) embedded in the *n*-octanethiolate matrix. The *n*-octanethiolate-covered Au(111) sample was immersed for 2 h at 23 °C in 0.1 mM catalyst **12** solution in ethanol. All images are 30 nm × 30 nm, and the tunneling parameters are −0.9 V and 13 pA. The time difference between two images is 4 min. The black arrows mark the same position on the sample. Because of thermal and piezoelectric drift, the imaged sample area shifts toward the bottom. This shift was corrected between image (d) and (e).

of the anion and the cationic headgroup, which is continuously changing. In conclusion, we assume that the observed blinking behavior of the functionalized thiolate **12** originates from structural fluctuations of the flexible ionic headgroup, which result in a different interaction with the tip from one scan to the other. The aforementioned explanation of Donhauser and co-workers³⁵ seems less likely in our case because it would predict similar behavior for the structurally related thiolate **18**, which, however, shows no blinking phenomenon.

Conclusions

We have developed a method for the incorporation of chiral rhodium-diphosphine complexes into self-assembled thiolate

monolayers on gold colloids by the place-exchange reaction. Our results show that these functionalized colloids, coated with a mixed monolayer of *n*-octanethiolates and thiolates with chiral rhodium-diphosphine end groups, possess catalytic properties comparable to analogous homogeneous rhodium catalysts. In the hydrogenation of methyl α -acetamidocinnamate, the same enantioselectivities (up to 93% ee) and full conversion could be obtained as with the corresponding homogeneous [Rh(COD)-(PYRPHOS)]BAR_F catalyst. The colloids could be easily recovered by filtration and reused as catalysts three times without loss of enantioselectivity. STM studies of analogous mixed SAMs on Au(111), prepared in the same manner, showed that the catalyst-bearing thiolates are distributed statistically on

the surface and that the ordered structure of the *n*-octanethiolate SAM can be retained during incorporation of the functionalized thiols. We are currently varying the structure of the components of the mixed SAMs, to study the influence of the neighboring thiolate molecules on the reactivity and enantioselectivity of the rhodium catalyst. In the systems investigated up to now, the thiolate linker attached to the rhodium complex extends beyond the surface of the SAM and, therefore, is exposed to the solvent. It will be interesting to see how systems in which the rhodium center is located inside the SAM behave.

Experimental Section

General Methods. Reactions with air- or moisture-sensitive compounds were performed under argon using standard Schlenk techniques or under purified N₂ in a MBraun glovebox. Glassware was oven-dried and flame-dried prior to use. All chemicals were purchased from Fluka or Aldrich. CH₂Cl₂ was dried over CaH₂ and THF over Na/K and freshly distilled under a stream of nitrogen prior to use. Optical rotations were measured in a Perkin-Elmer polarimeter 341, sodium lamp, 1 dm cuvette length, *c* in g/100 mL. ¹H, ¹³C, ¹⁹F, and ³¹P NMR spectra were recorded in CD₂Cl₂ or CDCl₃ on a Bruker Avance 400 or 500 MHz spectrometer, and coupling constants are reported in Hz. Chemical shifts are given in ppm relative to TMS. IR spectra: 1600 Perkin-Elmer Series FT-IR spectrometer. FAB mass spectra: Finnigan MAT 312. EI mass spectra: VG 70 SE. Elemental analyses were carried out on Leco CHN-900 and Leco RO-478 instruments. Chromatographic purifications were performed by flash chromatography using silica gel (Merck 0.040–0.063 mm). Yields for final products refer to isolated products and are the average of three runs. GC analyses: Carlo Erba HRGC Mega2 Series MFC 800 (column: Restek Rtx-1701; 0.25 mm, 30 m, 60 kPa He). HPLC analyses: Shimadzu VP-system (column: Daicel OD-H; 4.6 × 250 mm).

Disulfide 1. Oxalyl chloride (1.50 mL, 17.7 mmol) was added at 0 °C to a solution of 11-(10'-carboxydecylsulfanyl)undecanoic acid (2.20 g, 5.00 mmol) in freshly distilled dichloromethane (80 mL). The solution was stirred for 12 h at 23 °C. The solvent was concentrated under reduced pressure and the residue redissolved in freshly distilled dichloromethane, which was then added at 0 °C to a solution of PYRPHOS¹⁰ (4.60 g, 10.5 mmol) and triethylamine (3.00 mL, 21.6 mmol) in freshly distilled CH₂Cl₂ (100 mL) and stirred for 12 h at 23 °C. The resulting reaction mixture was washed with a NaOH solution (0.1 M, 100 mL) and water (100 mL). The organic phase was dried over MgSO₄, filtered, and concentrated under reduced pressure. Purification of the crude material by flash chromatography, eluting with 50% AcOEt in hexanes, gave 72% yield of the desired disulfide **1** (4.60 g). Mp: 46–48 °C. [α]_D²⁰ +80.1 (*c* 0.85, CHCl₃). *R*_f = 0.70 (hexanes/AcOEt, 1:1). ¹H NMR (400.1 MHz, CD₂Cl₂, 295 K): δ 1.26 (s_b, 6 H, CH₂), 1.29 (s_b, 4 H, CH₂), 1.37 (m_c, 2 H, CH₂CH₂CH₂S), 1.52 (m_c, 2 H, COCH₂CH₂), 1.66 (quin, *J* = 7.4 Hz, 2 H, CH₂CH₂S), 2.08 (t, *J* = 7.6 Hz, 2 H, COCH₂), 2.68 (t, *J* = 7.4 Hz, 2 H, CH₂S), 2.87 (m_c, 1 H, PCH), 2.95 (m_c, 1 H, PCH), 3.33 (t, *J* = 11.8 Hz, 1 H, NCH₂), 3.55 (t, *J* = 13.0 Hz, 1 H, NCH₂), 3.81 (m_c, 1 H, NCH₂), 3.89 (m_c, 1 H, NCH₂), 7.12–7.17 (m, 4 H, CH_{Ph}), 7.20–7.27 (m, 4 H, CH_{Ph}), 7.32–7.40 (m, 12 H, CH_{Ph}). ¹³C{¹H} NMR (100.6 MHz, CD₂Cl₂, 295 K): δ = 24.9 (COCH₂CH₂), 28.6 (CH₂CH₂CH₂S), 29.3 (CH₂), 29.3 (CH₂), 29.4 (CH₂), 29.5 (CH₂), 29.5 (CH₂), 29.5 (CH₂), 34.6 (COCH₂), 37.2 (m_c, *J*_{P,C} = 14 Hz, PCH), 39.1 (m_c, *J*_{C,P} = 14 Hz, PCH), 39.2 (CH₂S), 47.9 (m_c, NCH₂), 48.7 (m_c, NCH₂), 128.6–129.6 (m, CH_{Ph-ortho} and *para*), 133.4–133.8 (m, CH_{Ph-meta}), 135.9–136.7 (m, C_{Ph-*ipso*}), 171.5 (CO). ³¹P{¹H} NMR (162.0 MHz, CD₂Cl₂, 295 K): δ -12.5 (d, *J* = 8 Hz), -12.3 (d, *J* = 8 Hz). IR (KBr): ν (cm⁻¹) 3051w, 2923s, 2850m, 1644s, 1433s, 1197m, 1116m, 1095m, 743m, 696s, 506m. MS (FAB): *m/z* (rel int %) 1277 (M⁺, 2), 638 (12), 456 (10), 262 (11), 254 (9), 201 (23), 185 (98), 108 (12), 68 (100), 55 (27), 41(24).

Disulfide 4. Oxalyl chloride (1.50 mL, 17.7 mmol) was added at 0 °C to a solution of 11-(10'-carboxydecylsulfanyl)undecanoic acid (2.20 g, 5.00 mmol) in freshly distilled CH₂Cl₂ (80 mL). The solution was stirred for 12 h at 23 °C. The solvent was concentrated under reduced pressure and the residue redissolved in freshly distilled CH₂Cl₂ (50 mL), which was then added at 0 °C to a solution of *p*-nitrophenol (1.40 g, 10.0 mmol) and pyridine (0.80 mL, 10.0 mmol) in freshly distilled CH₂Cl₂ (100 mL) and stirred for 12 h at 23 °C. The resulting reaction mixture was washed with a HCl solution (0.1 M, 100 mL) and water (100 mL). The organic phase was dried over MgSO₄, filtered, and concentrated under reduced pressure. Purification of the crude material by flash chromatography, eluting with 20% AcOEt in hexanes, gave 85% yield of the desired disulfide **4** (2.91 g). Mp: 58–60 °C. *R*_f = 0.48 (hexanes/AcOEt, 5:1). ¹H NMR (400.1 MHz, CD₂Cl₂, 295 K): δ 1.30 (s_b, 16 H, CH₂), 1.37 (m_c, 8 H, CH₂), 1.65 (quin, *J* = 7.5 Hz, 4 H, SCH₂CH₂), 1.73 (quin, *J* = 7.5 Hz, 4 H, COCH₂CH₂), 2.58 (t, *J* = 7.5 Hz, 4 H, COCH₂), 2.67 (t, *J* = 7.5 Hz, 4 H, SCH₂), 7.27 (d, *J* = 9.1 Hz, 4 H, CO₂CCH_{Ar}), 8.24 (d, *J* = 9.1 Hz, 4 H, NO₂CCH_{Ar}). ¹³C{¹H} NMR (100.6 MHz, CD₂Cl₂, 295 K): δ 24.8 (CH₂), 28.5 (CH₂), 29.1 (CH₂), 29.3 (CH₂), 29.3 (CH₂), 29.3 (CH₂), 29.5 (CH₂), 34.3 (CH₂), 39.2 (SCH₂), 122.6 (CO₂CCH_{Ar}), 125.2 (NO₂CCH_{Ar}), 145.3 (NO₂C_{Ar}), 155.7 (CO₂C_{Ar}), 171.4 (CO₂). IR (KBr): ν (cm⁻¹) = 3100w, 2923s, 2851s, 1756s, 1620m, 1593m, 1525s, 1490m, 1471m, 1412w, 1344s, 1283m, 1208s, 1124s_b, 1012m, 923m, 866m, 717m, 495m. MS (FAB): *m/z* (rel int %) 676 (M⁺, 23), 538 (26), 399 (7), 232 (7), 171 (25), 140 (53), 115 (7), 101 (19), 97 (15), 87 (54), 83 (37), 69 (60), 55 (100), 41 (60). Anal. Calcd for C₃₄H₄₈N₂O₈S₂: C, 60.33; H, 7.15; N, 4.14; O, 18.91. Found: C, 60.44; H, 7.05; N, 4.03; O, 18.84.

4-Nitrophenyl 11-Mercaptoundecanoate (5). 1-Ethyl-3-(3'-dimethylaminopropyl)carbodiimide hydrochloride (3.16 g, 16.5 mmol) and *N*-hydroxybenzotriazole (2.23 g, 16.5 mmol) were added to a solution of 11-mercaptoundecanoic acid (3.00 g, 13.7 mmol) in freshly distilled CH₂Cl₂ (150 mL) at 0 °C. After 5 min, *p*-nitrophenol (1.91 g, 13.7 mmol) and pyridine (4.00 mL, 49.5 mmol) were added, and the reaction mixture was stirred for 6 h at 23 °C. The resulting solution was washed with a HCl solution (1 M, 100 mL) and water (100 mL). The organic phase was dried over MgSO₄, filtered, and concentrated under reduced pressure. Purification of the crude material by flash chromatography, eluting with 25 vol % AcOEt in hexanes, gave 63% yield of 4-nitrophenyl 11-mercaptoundecanoate **5** (2.90 g). Mp: 38–40 °C. *R*_f = 0.55 (hexanes/AcOEt, 4:1). ¹H NMR (400.1 MHz, CDCl₃, 295 K): δ 1.32 (t, *J* = 7.4 Hz, 1 H, SH), 1.35 (m_c, 12 H, CH₂), 1.59 (quin, *J* = 7.4 Hz, 2 H, HSCH₂CH₂), 1.74 (quin, *J* = 7.4 Hz, 2 H, COCH₂CH₂), 2.50 (q, *J* = 7.4 Hz, 2 H, HSCH₂), 2.58 (t, *J* = 7.4 Hz, 2 H, COCH₂), 7.26 (d, *J* = 9.1 Hz, 2 H, CO₂CCH_{Ar}), 8.25 (d, *J* = 9.1 Hz, 2 H, NO₂-CCH_{Ar}). ¹³C{¹H} NMR (100.6 MHz, CDCl₃, 295 K): δ 24.6 (CH₂), 24.7 (CH₂), 28.4 (CH₂), 29.0 (CH₂), 29.1 (CH₂), 29.2 (CH₂), 29.3 (CH₂), 29.4 (CH₂), 34.0 (CH₂), 34.3 (CH₂), 122.5 (CO₂CCH_{Ar}), 125.2 (NO₂CCH_{Ar}), 145.2 (NO₂C_{Ar}), 155.5 (CO₂C_{Ar}), 171.3 (CO₂). IR (KBr): ν (cm⁻¹) 3117w, 3083w, 2921s, 2851s, 1754s, 1620m, 1592m, 1535m, 1487m, 1413w, 1348s, 1202m, 1138s, 1010w, 923m, 860m, 716m, 492m. MS (FAB): *m/z* (rel int %) 340 ([M + H]⁺, 7), 201 (100), 140 (43), 123 (23), 97 (16), 83 (44), 69 (51), 55 (90), 41 (64). Anal. Calcd for C₁₇H₂₅NO₄S: C, 60.15; H, 7.42; N, 4.13; O, 18.85. Found: C, 60.17; H, 7.45; N, 4.13; O, 18.92.

Thiol 11. 1-Ethyl-3-(3'-dimethylaminopropyl)carbodiimide hydrochloride (0.96 g, 5.00 mmol) and *N*-hydroxybenzotriazole (0.68 g, 5.00 mmol) were added to a solution of 11-mercaptoundecanoic acid (1.15 g, 5.00 mmol) in freshly distilled CH₂Cl₂ (80 mL) at 0 °C. After 5 min, PYRPHOS¹⁰ (1.85 g, 4.20 mmol) and triethylamine (1.50 mL, 10.8 mmol) were added, and the reaction mixture was stirred for 6 h at 23 °C. The resulting solution was washed with a HCl solution (1 M, 100 mL) and water (100 mL). The organic phase was dried over MgSO₄, filtered, and concentrated under reduced pressure. Purification of the crude material by flash chromatography, eluting with 50% diethyl

ether in *n*-pentane, gave 86% yield of thiol **11** (2.30 g). Mp: 92–93 °C. $[\alpha]_D^{20} +125.8$ (*c* 0.93, CHCl_3). $R_f = 0.36$ (*n*-pentane/diethyl ether, 1:1). $^1\text{H NMR}$ (500.1 MHz, CD_2Cl_2 , 295 K): δ 1.27 (s_b, 12 H, CH_2), 1.37 (t, $^3J_{\text{H,H}} = 7.6$ Hz, 1 H, *SH*), 1.53 (m_c, 2 H, CH_2), 1.60 (quin, $^3J_{\text{H,H}} = 7.3$ Hz, 2 H, $\text{CH}_2\text{CH}_2\text{SH}$), 2.09 (t, $^3J_{\text{H,H}} = 7.7$ Hz, 2 H, COCH_2), 2.52 (dt, $^3J_{\text{H,H}} = 7.3$ Hz, 7.6 Hz, 2 H, CH_2SH), 2.87 (m_c, 1 H, *PCH*), 2.94 (m_c, 1 H, *PCH*), 3.34 (t, $^3J_{\text{H,H}} = 11.9$ Hz, 1 H, NCH_2), 3.67 (t, $^3J_{\text{H,H}} = 13.0$ Hz, 1 H, NCH_2), 3.90 (m_c, 1 H, NCH_2), 3.94 (m_c, 1 H, NCH_2), 7.13–7.19 (m, 4 H, CH_{Ph}), 7.21–7.28 (m, 4 H, CH_{Ph}), 7.32–7.45 (m, 12 H, CH_{Ph}). $^{13}\text{C}\{^1\text{H}\}$ NMR (125.8 MHz, CD_2Cl_2 , 295 K): δ 24.7 (CH_2), 24.9 (CH_2), 28.5 (CH_2), 29.1 (CH_2), 29.5 (CH_2), 29.5 (CH_2), 31.0 (CH_2), 31.0 (CH_2), 34.2 (CH_2), 34.8 (CH_2), 37.3 (m_c, *PCH*), 39.2 (m_c, *PCH*), 47.9 (m_c, NCH_2), 48.8 (m_c, NCH_2), 128.6–129.6 (m, $\text{CH}_{\text{Ph-ortho}}$ and *para*), 133.5–133.7 (m, $\text{CH}_{\text{Ph-meta}}$), 135.9–136.8 (m, $\text{C}_{\text{Ph-ipso}}$), 171.5 (CO). $^{31}\text{P}\{^1\text{H}\}$ NMR (202.5 MHz, CD_2Cl_2 , 295 K): δ -12.5 (d, $^3J_{\text{P,P}} = 8$ Hz), -12.3 (d, $^3J_{\text{P,P}} = 8$ Hz). IR (KBr): ν (cm^{-1}) 3053w, 2926s, 2847s, 1643s, 1432s, 1332m, 1270w, 1246w, 1214m, 1197w, 1090m, 1068m, 1025m, 999m, 739s, 702s, 646m, 543w, 513m, 482m. MS (EI): *m/z* (rel int %) 639 (M^+ , 16), 530 (13), 371 (11), 268 (13), 262 (64), 236 (7), 185 (47), 108 (16), 68 (100), 55 (12). Anal. Calcd for $\text{C}_{39}\text{H}_{47}\text{NOP}_2\text{S}$: C, 73.21; H, 7.40; N, 2.19; Found: C, 73.12; H, 7.36; N, 2.15.

Synthesis of Rhodium Complex 12. $[\text{Rh}(\text{COD})\text{Cl}]_2$ (0.89 g, 1.80 mmol) and $\text{TIBA}_{\text{Rf}}^{11,12}$ (3.84 g, 3.60 mmol) were dissolved in freshly distilled CH_2Cl_2 (50 mL) and stirred for 1 h at 23 °C. The precipitated TiCl_4 was filtered off and washed with freshly distilled CH_2Cl_2 (10 mL). To the resulting orange solution was added at 0 °C slowly a solution of thiol **11** (2.30 g, 3.60 mmol) in freshly distilled CH_2Cl_2 (20 mL) and stirred for 1 h at 23 °C. The solvent was concentrated at reduced pressure. The residue was purified by chromatography on silica gel, eluting with CH_2Cl_2 to provide the desired orange complex **12** (3.18 g) in 52% yield. Mp: 114–116 °C. $[\alpha]_D^{20} -25.8$ (*c* 0.24, CHCl_3). $R_f = 0.39$ (CH_2Cl_2). $^1\text{H NMR}$ (500.1 MHz, CD_2Cl_2 , 295 K): δ 1.19 (m_c, 10 H, CH_2), 1.33 (quin, $^3J_{\text{H,H}} = 7.3$ Hz, 2 H, $\text{CH}_2\text{CH}_2\text{CH}_2\text{SH}$), 1.36 (t, $^3J_{\text{H,H}} = 7.3$ Hz, 1 H, *SH*), 1.40 (quin, $^3J_{\text{H,H}} = 7.3$ Hz, 2 H, COCH_2CH_2), 1.63 (quin, $^3J_{\text{H,H}} = 7.3$ Hz, 2 H, $\text{CH}_2\text{CH}_2\text{SH}$), 1.94 (m_c, 2 H, COCH_2), 2.13 (m_c, 4 H, $\text{CH}_2\text{-COD}$), 2.43 (m_c, 2 H, $\text{CH}_2\text{-COD}$), 2.54 (m_c, 2 H, $\text{CH}_2\text{-COD}$), 2.65 (q, $^3J_{\text{H,H}} = 7.3$ Hz, 2 H, CH_2SH), 2.81 (m_c, 1 H, NCH_2), 2.94 (m_c, 1 H, NCH_2), 3.02 (m_c, 1 H, *PCH*), 3.12 (m_c, 1 H, *PCH*), 3.59 (m_c, 1 H, NCH_2), 3.83 (m_c, 1 H, NCH_2), 4.52 (m_c, 1 H, CH_{COD}), 4.56 (m_c, 1 H, CH_{COD}), 5.20 (m_c, 1 H, CH_{COD}), 5.23 (m_c, 1 H, CH_{COD}), 7.42 (m_c, 4 H, $\text{CH}_{\text{Ph-ortho}}$), 7.55 (m_c, 4 H, $\text{CH}_{\text{Ph-meta}}$), 7.56 (s_{br}, 4 H, $\text{CH}_{\text{Ph-para-BArF}}$), 7.58 (m_c, 2 H, $\text{CH}_{\text{Ph-para}}$), 7.64 (m_c, 4 H, $\text{CH}_{\text{Ph-meta}}$), 7.70 (m_c, 2 H, $\text{CH}_{\text{Ph-para}}$), 7.75 (s_b, 8 H, $\text{CH}_{\text{Ph-ortho-BArF}}$), 7.92 (m_c, 4 H, $\text{CH}_{\text{Ph-ortho}}$). $^{13}\text{C}\{^1\text{H}\}$ NMR (125.8 MHz, CD_2Cl_2 , 295 K): δ 24.7 (COCH_2CH_2), 28.6 ($\text{CH}_2\text{-COD}$), 28.8 ($\text{CH}_2\text{CH}_2\text{CH}_2\text{SH}$), 29.4 ($\text{CH}_2\text{CH}_2\text{SH}$), 29.5 (CH_2), 29.6 (CH_2), 29.7 (CH_2), 29.8 (CH_2), 32.2 ($\text{CH}_2\text{-COD}$), 34.3 (COCH_2), 39.3 (CH_2SH), 41.7 (ddd, $J = 2$ Hz, 18 Hz, 32 Hz, *PCH*), 43.2 (ddd, $J = 2$ Hz, 19 Hz, 32 Hz, *PCH*), 43.4 (m_c, $J_{\text{P,C}} = 4$ Hz, 17 Hz, NCH_2), 44.4 (dd, $J_{\text{P,C}} = 4$ Hz, 16 Hz, NCH_2), 98.6 (dd, $J_{\text{P,C}} = 7$ Hz, 8 Hz, CH_{COD}), 98.7 (dd, $J_{\text{P,C}} = 7$ Hz, 8 Hz, CH_{COD}), 104.8 (dd, $J_{\text{P,C}} = 7$ Hz, 9 Hz, CH_{COD}), 104.9 (dd, $J_{\text{P,C}} = 7$ Hz, 9 Hz, CH_{COD}), 117.9 (sept, $^3J_{\text{F,C}} = 4$ Hz, $\text{CH}_{\text{Ph-para-BArF}}$), 124.9 (q, $^1J_{\text{F,C}} = 272$ Hz, $\text{CF}_3\text{-BArF}$), 126.2 (d, $^1J_{\text{P,C}} = 42$ Hz, $\text{C}_{\text{Ph-ipso}}$), 126.3 (d, $^1J_{\text{P,C}} = 43$ Hz, $\text{C}_{\text{Ph-ipso}}$), 127.7 (d, $^1J_{\text{P,C}} = 44$ Hz, $\text{C}_{\text{Ph-ipso}}$), 127.8 (d, $^1J_{\text{P,C}} = 44$ Hz, $\text{C}_{\text{Ph-ipso}}$), 129.2 (q, $^2J_{\text{F,C}} = 31$ Hz, $^3J_{\text{B,C}} = 3$ Hz, CCF_3), 130.4 (d, $^3J_{\text{P,C}} = 12$ Hz, $\text{CH}_{\text{Ph-meta}}$), 130.5 (d, $^3J_{\text{P,C}} = 12$ Hz, $\text{CH}_{\text{Ph-meta}}$), 130.6 (d, $^3J_{\text{P,C}} = 16$ Hz, $\text{CH}_{\text{Ph-meta}}$), 130.7 (d, $^3J_{\text{P,C}} = 16$ Hz, $\text{CH}_{\text{Ph-meta}}$), 132.2 (d, $^4J_{\text{P,C}} = 2.4$ Hz, $\text{CH}_{\text{Ph-para}}$), 133.8 (d, $^4J_{\text{P,C}} = 2.4$ Hz, $\text{CH}_{\text{Ph-para}}$), 135.2 (m_b, $\text{CH}_{\text{Ph-ortho-BArF}}$), 136.9 (d, $^2J_{\text{P,C}} = 21$ Hz, $\text{CH}_{\text{Ph-ortho}}$), 137.0 (d, $^2J_{\text{P,C}} = 21$ Hz, $\text{CH}_{\text{Ph-ortho}}$), 162.1 (q, $^1J_{\text{B,C}} = 50$ Hz, $\text{C}_{\text{Ph-ipso-BArF}}$), 172.1 (CO). $^{31}\text{P}\{^1\text{H}\}$ NMR (202.5 MHz, CD_2Cl_2 , 295 K): δ 30.1 (dd, $^1J_{\text{P,Rh}} = 149$ Hz, $^2J_{\text{P,P}} = 28$ Hz, P), 31.1 (dd, $^1J_{\text{P,Rh}} = 149$ Hz, $^2J_{\text{P,P}} = 28$ Hz, P). $^{19}\text{F}\{^1\text{H}\}$ NMR (470.6 MHz, CD_2Cl_2 , 295 K): δ -63.9 (s). IR (KBr): ν (cm^{-1}) 2929m, 1653s, 1430m_b, 1356s, 1278s, 1127s_b, 889m, 839w, 745m, 694m_b, 522m. MS (FAB): *m/z* (rel int %) 850

($[\text{M} - \text{BArF}]^+$, 22), 738 (24), 540 (18), 474 (17), 395 (22), 317 (42), 286 (53), 255 (26), 241 (46), 210 (100), 183 (30), 103 (37), 89 (26), 77 (40), 68 (58), 55 (30), 39 (38). Anal. Calcd for $\text{C}_{79}\text{H}_{71}\text{NOBF}_2\text{P}_2$ -*RhS*: C, 55.36; H, 4.18; N, 0.82; O, 0.93. Found: C, 55.25; H, 4.12; N, 0.81; O, 1.02.

Thiol 18. 1-Ethyl-3-(3'-dimethylaminopropyl)carbodiimide hydrochloride (0.91 g, 4.77 mmol) and *N*-hydroxybenzotriazole (0.64 g, 4.77 mmol) were added to a solution of 11-mercaptoundecanoic acid (1.00 g, 4.70 mmol) in freshly distilled CH_2Cl_2 (100 mL) at 0 °C. After 5 min, (3*R*,4*R*)-3,4-bis(diphenylphosphorothioyl)pyrrolidine (2.00 g, 3.97 mmol) and triethylamine (1.80 mL, 12.8 mmol) were added, and the reaction mixture was stirred for 6 h at 23 °C. The resulting solution was washed with a saturated NH_4Cl solution (100 mL) and water (100 mL). The organic phase was dried over MgSO_4 , filtered, and concentrated under reduced pressure. Purification of the crude material by flash chromatography, eluting with 30% diethyl ether in *n*-pentane, gave 80% yield of thiol **18** (2.24 g). Mp: 62–64 °C. $[\alpha]_D^{20} +26.3$ (*c* 0.83, CHCl_3). $R_f = 0.26$ (*n*-pentane/diethyl ether, 1:2). $^1\text{H NMR}$ (500.1 MHz, CDCl_3 , 295 K): δ 1.16–1.29 (m, 10 H, CH_2), 1.33 (t, $J = 7.6$ Hz, 1 H, *SH*), 1.31–1.39 (m, 2 H, CH_2), 1.48 (quin_b, $J = 7.0$ Hz, 2 H, CH_2), 1.59 (quin, $J = 7.4$ Hz, 2 H, $\text{CH}_2\text{CH}_2\text{SH}$), 1.93 (m_c, 2 H, COCH_2), 2.51 (m_c, $J = 7.1$ Hz, 7.6 Hz, 2 H, CH_2SH), 3.55–3.64 (m, 1 H, *PCH*), 3.74–3.83 (m, 2 H, NCH_2), 3.84–3.93 (m, 1 H, *PCH*), 3.96–4.10 (m, 2 H, NCH_2), 7.21–7.28 (m, 4 H, CH_{Ph}), 7.36–7.53 (m, 8 H, CH_{Ph}), 7.60–7.66 (m, 2 H, CH_{Ph}), 7.71–7.76 (m, 2 H, CH_{Ph}), 7.79–7.87 (m, 4 H, CH_{Ph}). $^{13}\text{C}\{^1\text{H}\}$ NMR (125.8 MHz, CDCl_3 , 295 K): δ 24.9 (CH_2), 25.0 (CH_2), 28.7 (CH_2), 29.4 (CH_2), 29.6 (CH_2), 29.7 (CH_2), 29.7 (CH_2), 29.8 (CH_2), 34.4 (CH_2), 34.7 (CH_2), 38.7 (d, $J_{\text{C,P}} = 54$ Hz, *PCH*), 39.9 (d, $J_{\text{C,P}} = 54$ Hz, *PCH*), 48.1 (s, NCH_2), 48.4 (s, NCH_2), 129.1–129.3 (m, $\text{CH}_{\text{Ph-meta}}$), 129.6–131.3 (m, $\text{C}_{\text{Ph-ipso}}$), 131.7–132.4 (m, $\text{CH}_{\text{Ph-ortho}}$ and *para*), 171.5 (CO). $^{31}\text{P}\{^1\text{H}\}$ NMR (202.5 MHz, CDCl_3 , 295 K): δ 50.8 (d, $J = 41$ Hz), 51.0 (d, $J = 41$ Hz). IR (KBr): ν (cm^{-1}) 2924s, 2851m, 1639s, 1436s, 1100s, 750m, 713s, 692s, 608m, 520m, 489m. MS (FAB): *m/z* (rel int %) 704 ($[\text{M} + \text{H}]^+$, 9), 268 (8), 217 (16), 136 (9), 68 (100), 57 (13), 41 (10). Anal. Calcd for $\text{C}_{39}\text{H}_{47}\text{NOP}_2\text{S}_2$: C, 66.54; H, 6.73; N, 1.99; O, 2.27. Found: C, 66.45; H, 6.62; N, 1.92; O, 2.35.

General Procedure for the Synthesis of Functionalized Gold Particles. Gold particles and all glassware used for the preparation and storage of gold particles was treated with aqua regia, rinsed with deionized water, cleaned in a bath consisting of seven parts of concentrated sulfuric acid and three parts of 30% hydrogen peroxide (*piranha* solution), rinsed again with deionized water, and dried for 12 h at 120 °C. All reactions were carried out under argon.

Freshly cleaned gold particles (0.50 g) were transferred into a 10 mL gastight SGE syringe (fitted with a push button luer lock valve and an integrated filter), containing a solution of the desired disulfide (0.05 mmol) in freshly distilled CH_2Cl_2 (4 mL). The syringe was shaken (80 rpm) under argon for 24 h at 23 °C. The functionalized gold particles were filtered in the syringe under argon, washed with freshly distilled CH_2Cl_2 (8×5 mL), and dried in vacuo for 1 h to give the functionalized gold particles.

$[\text{Rh}(\text{COD})\text{Cl}]_2$ (0.10 g, 0.20 mmol) and $\text{TIBA}_{\text{Rf}}^{11,12}$ (0.43 g, 0.40 mmol) were dissolved in freshly distilled CH_2Cl_2 (10 mL) and stirred for 1 h at 23 °C. The precipitated TiCl_4 was filtered off and washed with freshly distilled CH_2Cl_2 (2 mL). The resulting orange solution was transferred under argon into a 10 mL gastight SGE syringe (fitted with a push button luer lock valve and an integrated filter), containing the functionalized gold particles **2**. The syringe was shaken (80 rpm) under argon for 12 h at 23 °C. The functionalized gold particles were filtered in the syringe under argon, washed with freshly distilled CH_2Cl_2 (8×5 mL), and dried in vacuo for 1 h to give the functionalized gold particles **3**, which were immediately used for the asymmetric hydrogenation of methyl α -acetamidocinnamate.

General Procedure for the Synthesis of *n*-Alkanethiolate-Protected Gold Colloids. All glassware used for the preparation and

storage of colloidal Au was treated with aqua regia, rinsed with deionized water, cleaned in a bath consisting of seven parts of concentrated sulfuric acid and three parts of 30% hydrogen peroxide (*piranha* solution), rinsed again with deionized water, and dried for 12 h at 120 °C. All reactions were carried out under argon in the dark.

To a vigorously stirred solution (1200 rpm) of $\text{HAuCl}_4 \cdot (\text{H}_2\text{O})_x$ (3.00 g, ~49% Au, 1 equiv) in deionized H_2O (240 mL) was added a solution of tetraoctylammoniumbromide (4.50 g, 1.1 equiv) in freshly distilled toluene (165 mL). The yellow color of the gold acid solution quickly disappeared and the toluene phase became orange-red as the AuCl_4^- was transferred into it. The mixture was shaken several times until the aqueous phase became colorless. The organic phase was isolated, and *n*-octanethiol (0.26 mL, 0.20 equiv) was added to the solution. The resulting solution was cooled to 0 °C. Under vigorous stirring (1200 rpm) was subsequently added NaBH_4 (3.10 g, 11 equiv) in deionized water (200 mL). The colloids were transformed instantaneously, as witnessed by the color change of the solution from red to black. The very dark organic phase was further stirred for 12 h at 23 °C. The organic phase was collected and the solution concentrated to 20 mL at reduced pressure (the water bath should not exceed 30 °C to prevent partial product decomposition). The black product was suspended in ethanol (300 mL) and briefly sonicated to ensure complete dissolution of byproducts. The mixture was kept at -60 °C for 48 h to effect complete precipitation. The colloids were collected on a glass filtration frit and washed twice with ethanol (200 mL) and twice with acetone (200 mL). The black material was dried in vacuo for 1 h to give *n*-octanethiol-passivated gold nanoparticles (1.84 g), free of significant residual *n*-octanethiol. The absence of free *n*-alkanethiol was confirmed by ^1H NMR spectroscopy (CD_2Cl_2 , no $\alpha\text{-CH}_2$ resonance at ~2.5 ppm) and IR spectroscopy (no $\nu_{\text{asym}}(\text{SH})$ band in the region of 2576 cm^{-1}). On the basis of elemental analysis (C 7.15%, H 1.31%, S 2.38%, Au 90.1%), TEM ($3.48 \pm 0.61\text{ nm}$), and Leff's model,¹⁷ the colloids contained an average number of 1298 gold atoms/core and 211 adsorbed *n*-octanethiolate molecules.

Exchange Reaction on *n*-Alkanethiolate-Protected Gold Colloids.

To a solution of *n*-alkanethiol-protected gold colloids (0.80 g, ~0.6 mmol adsorbed *n*-alkanethiol, 1 equiv) in freshly distilled CH_2Cl_2 (400 mL) was added a solution of functionalized thiol (0.6 mmol, 1 equiv) in freshly distilled CH_2Cl_2 (100 mL), and the mixture was stirred (80 rpm) for 24–48 h at 23 °C. The solution was concentrated to 50 mL under reduced pressure (the water bath should not exceed 30 °C to prevent partial product decomposition), diluted with ethanol (300 mL), and briefly sonicated to ensure complete dissolution of byproducts. The colloids were collected by filtration with a solvent-resistant stirred cell (Millipore, 76 mm disk filter and a ultrafiltration membrane (regenerated cellulose, PLTK, NMWL: 30'000)) and washed with ethanol until the filtrate was colorless, indicating removal of all excess free thiol **12**. The black solution remaining in the stir cell was concentrated to 50 mL, suspended in hexanes (300 mL), and briefly sonicated to ensure complete dissolution of byproducts. The mixture was kept at -60 °C for 48 h to effect complete precipitation. The colloids were collected on a glass filtration frit and washed twice with hexanes (200 mL). The black material was dried in vacuo for 1 h to give the functionalized gold nanoparticles, which were analyzed by ^1H NMR and TEM.

Hydrogenation. The rhodium colloid catalyst (5 μmol , 1 mol %) and methyl α -acetamidocinnamate (110 mg, 0.50 mmol) were added to a borosilicate glass vial (30 \times 60 mm) in the glovebox. After addition of the appropriate solvent (1 mL) and a stirring bar (6 \times 15 mm), the vial was placed in an autoclave, which was pressurized with hydrogen at 60 bar. The reaction mixture was stirred (600 rpm) for 4 h at 23 °C. After the reaction, the hydrogen pressure was released, the solvent was removed, and the residue was purified on a short silica plug to remove the catalyst (6 \times 20 mm; eluting with ethyl acetate). The product was dissolved in ethanol and used directly for HPLC and GC analysis.

Catalyst Recycling. The autoclave was slowly opened in the fume

hood and the reaction solution treated immediately with 10 equiv of neat COD. The solution was diluted with 10 mL of ethyl acetate and transferred to a Millipore Centriplus centrifugal filter device with a cutoff molecular size of 50 kD. After centrifugation (3000 rpm) at 23 °C for 60 min, the filtrate containing the product was removed. The remaining colloid solution was diluted with ethyl acetate and centrifuged again. This procedure was repeated twice in order to remove any remaining product. The concentrated colloidal solution was transferred to a flask, concentrated to near dryness, and treated with hexanes to induce precipitation. The resulting suspension was cooled to -78 °C for 2 h. The black precipitate, which had formed, was isolated by filtration and washed with hexanes. The colloids were then dried under vacuum and reused as catalysts.

STM Investigations. Au(111) Substrate. The gold films were obtained by epitaxial growth of gold onto mica at a base pressure of 5×10^{-7} mbar while the substrate was held at 350 °C, similar to the procedure described in the literature.³⁶ Shortly before the preparation of the SAMs the gold substrates were either heated to 500 °C for 2 h in an oven or flame-annealed to remove contaminants.³⁷ The latter process turned out to be more reliable to give clean and smooth gold surfaces.

SAM Preparation. The gold films were immersed in a solution of *n*-octanethiols under argon atmosphere, whereas the immersion time (ranging from 3 to 24 h), the solvent (ethanol, dichloromethane, acetone, toluene, and diethyl ether), the concentration (ranging from 1 mM to 0.1 M), and the solution temperature (ranging from 23 to 60 °C) were varied in order to determine the best conditions for obtaining upright standing *n*-octanethiolate monolayers in the well-known ($\sqrt{3} \times \sqrt{3}$)-R30 hexagonal arrangement. Upon removal from solution, the samples were carefully rinsed with pure solvent.

Exchange Reaction. Only samples that showed the hexagonal ($\sqrt{3} \times \sqrt{3}$)-R30 *n*-octanethiolate ordering, which was checked with STM, were used to perform the exchange reaction. For this purpose, the samples were immersed in a 0.1–2 mM solution of either the ligand **18** or the ionic catalyst **12**. As solvent, ethanol or dichloromethane were used, while the immersion time was varied between 1 and 48 h. Long immersion times (~8 h) led to disruption of the hexagonal *n*-octanethiolate ordering by desorption of *n*-octanethiol. However, addition of *n*-octanethiol to the ligand **18** solution prevented this effect. For the exchange reaction with catalyst **12**, no *n*-octanethiol was added to the solution.

STM Measurements. The STM measurements were carried out at ambient conditions with a Nanoscope IIIa (Digital Instruments Inc., Santa Barbara, CA) equipped with a low-current converter. The tips were mechanically cut from a Pt/Ir wire (90:10). As typical scan parameters, $\pm 0.9\text{ V}$ and 2 pA were used for the bias voltage and the tunneling current, respectively.

Acknowledgment. Financial support by the Swiss National Science Foundation and the National Center of Competence in Research (NCCR) "Nanoscale Science" is gratefully acknowledged. M.S. acknowledges support from the German Academy of Natural Scientists Leopoldina under the grant number BMBF-LPD 9901/8-86.

Supporting Information Available: Full details of ligand/colloid synthesis and characterization as well as complete ref 13. This material is available free of charge via the Internet at <http://pubs.acs.org>.

JA0500714

- (36) DeRose, J. A.; Thundat, T.; Nagahara, L. A.; Lindsay, S. M. *Surf. Sci.* **1991**, *265*, 102.
(37) Dishner, M. H.; Ivey, M. M.; Gorer, S.; Hemminger, J. C.; Feher, F. J. *J. Vac. Sci. Technol. A* **1998**, *16*, 329.